THE JOURNAL OF BIOLOGICAL CHEMISTRY
Vol. 279, No. 9, Issue of February 27, pp. 8506–8515, 2004
Printed in U.S.A.
© 2004 by The American Society for Biochemistry and Molecular Biology, Inc.

Familial Parkinson's Disease-associated L166P Mutation Disrupts DJ-1 Protein Folding and Function*

Received for publication, October 7, 2003, and in revised form, December 5, 2003
Published, JBC Papers in Press, December 9, 2003, DOI 10.1074/jbc.M311017200

James A. Olzmann‡, Keith Brown‡, Keith D. Wilkinson§, Howard D. Rees¶, Qing Huai‖, Hengming Ke‖, Allan I. Levey¶, Lian Li‡, and Lih-Shen Chin‡**

From the Departments of ‡Pharmacology, §Biochemistry, and ¶Neurology, Center for Neurodegenerative Disease, Emory University School of Medicine, Atlanta, Georgia 30322-3090 and the ‖Department of Biochemistry and Biophysics, University of North Carolina, Chapel Hill, North Carolina 27599-7260

Mutations in DJ-1, a protein of unknown function, were recently identified as the cause for an autosomal recessive, early onset form of familial Parkinson's disease. Here we report that DJ-1 is a dimeric protein that exhibits protease activity but no chaperone activity. The protease activity was abolished by mutation of Cys-106 to Ala, suggesting that DJ-1 functions as a cysteine protease. Our studies revealed that the Parkinson's disease-linked L166P mutation impaired the intrinsic folding propensity of DJ-1 protein, resulting in a spontaneously unfolded structure that was incapable of forming a homodimer with itself or a heterodimer with wild-type DJ-1. Correlating with the disruption of DJ-1 structure, the L166P mutation abolished the catalytic function of DJ-1. Furthermore, as a result of protein misfolding, the L166P mutant DJ-1 was selectively polyubiquitinated and rapidly degraded by the proteasome. Together these findings provide insights into the molecular mechanism by which loss-of-function mutations in DJ-1 lead to Parkinson's disease.

Parkinson's disease (PD)[1] is an age-related neurodegenerative movement disorder characterized by the degeneration of dopaminergic neurons in the substantia nigra and the presence of intraneuronal inclusions known as Lewy bodies (1, 2). Although PD has been known for nearly 2 centuries, the molecular mechanisms underlying the pathogenesis of PD is not understood, and currently there is no treatment to stop the progression of this devastating disease. Recent evidence indicates that at least 10 distinct genetic loci, *PARK1–PARK10*, are linked to familial forms of PD (3, 4). The responsible genes for three of these loci, *PARK1*, *PARK2*, and *PARK5*, were found to encode α-synuclein (5), parkin (6), and ubiquitin carboxyl-terminal hydrolase L1 (7), respectively. Studies of these familial PD gene products have generated valuable insights into PD pathogenesis and led to the hypothesis that dysfunction in the ubiquitin-proteasome pathway may be a common mechanism leading to neurodegeneration in PD (8, 9).

Recently it was reported that mutations in DJ-1 underlie the *PARK7* loci for an autosomal recessive, early onset form of familial PD (10). To date, three PD-linked DJ-1 mutations have been identified: a homozygous 14-kb deletion (10) and a compound heterozygous mutation (11), both of which result in the loss of DJ-1 protein, and a homozygous missense mutation (L166P) that replaces Leu-166 with a proline in the DJ-1 protein (10). The complete cosegregation of these mutations with the PD allele suggests that loss of the normal function of DJ-1 causes this recessively transmitted PD (10).

DJ-1 is a ubiquitously expressed protein initially identified as an oncogene with transforming activity (12). A connection to cancer is also suggested by the identification of DJ-1 as a circulating tumor antigen in breast cancer (13). Human DJ-1 was independently described as RS, a regulatory subunit of a ~400-kDa RNA-binding protein complex (14). Rat DJ-1, also known as CAP-1 (15) and SP22 (16), has been linked to male infertility induced by exposure to sperm toxicants (17, 18). DJ-1 appears to regulate androgen receptor-mediated gene transcription via its interaction with PIASxα (protein inhibitor of activated STAT) and DJ-1-binding protein (19, 20). In addition, DJ-1 has been proposed to participate in the cellular defense against oxidative stress since it undergoes a pI shift from 6.2 to 5.8 upon treatment of cells with H_2O_2 or paraquat (21, 22). Despite these observations implicating DJ-1 in multiple cellular processes, the precise biochemical function of DJ-1 remains unknown.

DJ-1 is an evolutionarily conserved, 189-amino acid protein that exhibits significant sequence homology with the PfpI family of intracellular proteases (23) and with the ThiJ family of bacterial proteins involved in thiamin synthesis (24). We and other groups have recently solved the crystal structure of human DJ-1, which shows that DJ-1 adopts a helix-strand-helix sandwich structure similar to the bacterial protease PH1704 and *Escherichia coli* chaperone protein Hsp31 (25–29). However, it is unclear whether DJ-1 has a protease or chaperone function because the Cys-His-(Glu/Asp) catalytic triad and the quaternary structure of PH1704 and Hsp31 are not conserved in DJ-1. Furthermore the structural and functional consequences of the PD-associated L166P mutation remain to be defined. In the present study, we undertook the characterization of the molecular and biochemical properties of DJ-1 and investigated how the structure and function of DJ-1 are altered by the disease-linked L166P mutation.

* This work was supported by grants from the University Research Committee of Emory University and the Emory Collaborative Center (Grant ES012068) for Environmental Research on Parkinson's Disease (to L.-S. C.) and by National Institutes of Health Grants AG021489 and NS047199 and an Emory Center for Neurodegenerative Disease-Merck Scholar Award (to L. L.). The costs of publication of this article were defrayed in part by the payment of page charges. This article must therefore be hereby marked "*advertisement*" in accordance with 18 U.S.C. Section 1734 solely to indicate this fact.

** To whom correspondence should be addressed: Dept. of Pharmacology, Emory University School of Medicine, 1510 Clifton Rd., Atlanta, GA 30322-3090. Tel.: 404-727-5987; Fax: 404-727-0365; E-mail: lianli@pharm.emory.edu.

[1] The abbreviations used are: PD, Parkinson's disease; HA, hemagglutinin; GFP, green fluorescent protein; E3, ubiquitin-protein ligase; STAT, signal tranducers and activators of transcription.

This is an Open Access article under the CC BY license.

EXPERIMENTAL PROCEDURES

DJ-1 Expression Constructs—The DJ-1 cDNA corresponding to the entire coding region of human DJ-1 (12) was obtained by PCR. The L166P and C106A single and double mutant cDNAs were obtained by site-directed mutagenesis using a PCR overlap extension method (30). These cDNAs were analyzed on both strands by DNA sequencing to ensure there were no unwanted changes in the codons. The wild-type and mutant DJ-1 cDNAs were then used to make the following expression vectors: pCHA-DJ-1, pMyc-DJ-1, pGFP-DJ-1, and the corresponding L166P and C106A mutant forms, which allow the expression of amino-terminally HA-, Myc-, or GFP-tagged wild-type and mutant DJ-1 proteins in mammalian cells. All expression constructs were sequenced to confirm that the fusion was in the correct reading frame.

Antibodies—Two distinct rabbit polyclonal anti-DJ-1 antibodies, P7F and P7C, were generated against purified full-length recombinant human DJ-1 protein and a synthetic human DJ-1 carboxyl-terminal peptide ALNGKEVAAQVKAPLVLKD, respectively, using the same procedures as described previously (31). Other antibodies used in this study include the following: anti-HA (3F10, Roche Applied Science; HA.11, Covance), anti-Myc (9E10.3, Neomarkers), anti-actin (C4, Chemicon); and secondary antibodies coupled to horseradish peroxidase (Jackson ImmunoResearch Laboratories, Inc.).

Immunohistochemistry—Rats were perfused transcardially with 3% paraformaldehyde, and brain sections were cut at 50-μm thickness and stored in cryoprotectant until use. Sections were rinsed in phosphate buffer and pretreated for 1 h in a solution containing 8% goat serum, 10 μg/ml avidin, 0.1% Triton X-100, 0.9% NaCl, and 50 mM Tris-HCl (pH 7.2). Sections were then incubated for 48 h with rabbit polyclonal anti-DJ1 antibody P7F or P7C at 1:2000 followed by incubation with biotinylated goat anti-rabbit secondary antibody (1:200, Vector Laboratories). Immunoreactivity was visualized using the standard avidin-biotinylated peroxidase complex method (Vectastain Elite ABC kit, Vector Laboratories). For controls, sections were processed in parallel with primary antibody omitted or with excess amount of immunogens.

Protein Expression and Purification—Wild-type and mutant DJ-1 were expressed in BL21 *E. coli* cells as untagged proteins (25, 32) and purified by ammonium sulfate fractionation, Sepharose Q XL ion exchange chromatography, and Sephacryl S-100 gel filtration chromatography. Fractions containing DJ-1 were identified with SDS-PAGE and pooled for further studies. Protein concentration was determined by using the bicinchoninic acid (BCA) assay (Pierce).

Size Exclusion Chromatography—Purified wild-type or L166P mutant DJ-1 protein (1 ml at 10 mg/ml) was loaded on a HiPrep 16/60 Sephacryl S-100 high-resolution column and fractionated by size exclusion chromatography using an ΔKTAprime chromatography system (Amersham Biosciences). The column was eluted at 4 °C using a flow rate of 0.5 ml/min in a buffer containing 100 mM NaCl, 1 mM EDTA, 1 mM β-mercaptoethanol, and 20 mM Tris-HCl (pH 7.5), and 5-ml fractions were collected. The column was calibrated under identical running conditions with protein standards (Sigma), including blue dextran (2000 kDa), β-amylase (200 kDa), albumin (66 kDa), carbonic anhydrase (29 kDa), cytochrome *c* (12.4 kDa), and aprotinin (6.5 kDa).

CD Spectroscopy—Far UV CD spectra were obtained using an AVIV model 62DS CD spectrometer and a quartz cuvette with a path length of 0.1 or 1 cm. Spectra were recorded at 25 °C from 250 to 200 nm with a step size of 0.5 nm and a bandwidth of 1.5 nm, and an average of 10 scans was obtained. CD measurements were performed with purified, untagged wild-type or mutant DJ-1 proteins at a final concentration of 2–35 μM in a buffer containing 20 mM Tris-HCl (pH 7.4) and 100 mM NaCl. Mean residue ellipticity is defined as the observed ellipticity normalized by the molar concentration of amino acid residues in the indicated protein. Thermal denaturation was studied by measuring far UV CD in 1-cm cuvette at 222 nm while the temperature was increased from 5 °C to 90 °C with a step size of 2 °C. Melting temperature (T_m) is defined as the temperature at which 50% of the α-helical structure (measured by ellipticity at 222 nm) is denatured. Reversibility of thermal denaturation was assessed in the same cuvette at 222 nm while the temperature was cooled from 90 °C to 5 °C with a step decrease of 2 °C.

Chaperone Activity Assay—The potential chaperone function of DJ-1 was investigated by using a well established chaperone assay that measures the ability of a molecular chaperone to suppress the thermal aggregation of citrate synthase (33). To induce aggregation, 45 μM porcine heart citrate synthase (Sigma) was diluted 1:300 in 40 mM HEPES-KOH, pH 7.5 at 43 °C in the presence and absence of wild-type or mutant DJ-1. To monitor the kinetics of thermal aggregation, light scattering was measured in a PerkinElmer Life Sciences LS55 luminescence spectrometer in a stirred and thermostatted quartz cell. Both the excitation and emission wavelengths were set to 500 nm with a slit width of 2.5 nm. Recombinant murine heat shock protein Hsp25 (Stressgen) was used as a positive control for the chaperone assay.

Protease Activity Assays—Protease activity of DJ-1 and its mutants was measured by an in-gel protease assay and a continuous fluorescence-based protease assay. The in-gel protease assay was carried out as described previously for determining the protease activity of the PfpI family of proteases (34, 35). Purified wild-type or mutant DJ-1 protein (1–100 μg) was electrophoresed onto 12% SDS-polyacrylamide gels containing 0.1% co-polymerized gelatin under non-reducing conditions. After electrophoresis, the gels were washed in 2.7% Triton X-100 and then incubated overnight at 37 °C in 200 mM NaCl, 5 mM $CaCl_2$, and 50 mM Tris-HCl (pH 7.4). The gels were stained with Coomassie Brilliant Blue to visualize zones of gelatin hydrolysis. The fluorescence-based protease assays were performed as described previously (36) by using the EnzCheck protease assay kit (Molecular Probes). Purified wild-type or mutant DJ-1 (1–50 μM) was incubated with BODIPY FL-labeled casein (10 μg/ml) in 50 mM Tris-HCl, pH 7.4, 200 mM NaCl, and 5 mM $CaCl_2$ at 37 °C. An increase in fluorescence upon protease-catalyzed hydrolysis of BODIPY FL-casein was monitored continuously in a PerkinElmer Life Sciences LS55 luminescence spectrometer using an excitation wavelength of 505 nm and emission wavelength of 513 nm. Kinetic parameters (K_m and k_{cat}) were obtained as described previously (37) by fitting the data to the following equation: $v = k_{cat}\ [S]_0/(1 + K_m[E]^{-1})$. Trypsin (Athena Environmental Sciences, Inc.) was used as a positive control for both in-gel and fluorescence-based protease assays.

Cell Transfections and Immunoprecipitations—HeLa or SH-SY5Y cells were transfected with the indicated plasmids using LipofectAMINE (Invitrogen) as described by the manufacturer. Stable transfectants were isolated in selection medium containing 0.5 mg/ml G418 (Invitrogen), and ~300 colonies were pooled for further studies. Cell lysates were prepared from transfected cells and subjected to immunoprecipitation as described previously (38) using anti-HA antibody (3F10). The immunocomplexes were recovered by incubation with protein G-Sepharose beads (Sigma). After extensive washes, the immunocomplexes were dissociated by boiling in the Laemmli sample buffer and analyzed by SDS-PAGE and immunoblotting with appropriate primary and secondary antibodies. Antibody binding was visualized by using the enhanced chemiluminescence system (Amersham Biosciences).

Proteolysis Inhibitor Treatment of Cells—HeLa or SH-SY5Y cells expressing wild-type or L166P mutant DJ-1 were incubated for 8 h at 37 °C with the proteasome inhibitor MG132 (20 μM, Calbiochem), the lysosomal protease inhibitor chloroquine (100 μM, Sigma), or vehicle (dimethyl sulfoxide (Me_2SO); final concentration, 0.1%). Cells were then lysed, and an equal amount of proteins from each lysate was analyzed by immunoblotting for HA-tagged DJ-1 and actin. The relative level of wild-type or mutant DJ-1 was quantified by using the NIH Image program and normalized against the level of actin. Statistical analyses were performed by the unpaired Student's *t* test.

Ubiquitination Assays—In vivo ubiquitination assays were performed as described previously (39, 40). Briefly HeLa cells were transfected with pcDNA3-myc-ubiquitin in combination with pCHA-DJ-1 or pCHA-L166P. Twenty-four hours after transfection, the cells were incubated for 8 h with vehicle control (0.1% Me_2SO) or proteasome inhibitor MG132 (20 μM in Me_2SO). The cells were then lysed, and an equal amount of proteins from each lysate was subjected to immunoprecipitation using anti-HA antibodies. Immunoprecipitates were analyzed by SDS-PAGE followed by immunoblotting with an anti-Myc antibody to detect Myc-ubiquitin conjugated to wild-type or L166P mutant DJ-1.

[^{35}S]Methionine Pulse-Chase Experiments—Pulse-chase experiments were performed as described previously (39, 40). SH-SY5Y cells stably transfected with pCHA-DJ-1 or pCHA-L166P were labeled by incubation for 1 h with Met/Cys-free Dulbecco's modified Eagle's medium containing 100 μCi of [^{35}S]Met/Cys (1000 Ci/mmol) express protein labeling mixture (PerkinElmer Life Sciences). After extensive washes, cells were incubated for the indicated chase time in non-radioactive Dulbecco's modified Eagle's medium supplemented with 10% fetal bovine serum and 5 times the normal concentration of methionine and cysteine. Cells were then lysed, and an equal amount of proteins from each lysate was immunoprecipitated using an anti-HA antibody. Immunoprecipitates were resolved by SDS-PAGE and analyzed by a PhosphorImager (Amersham Biosciences).

RESULTS

Generation of Anti-DJ-1 Antibodies and Characterization of DJ-1 Protein Expression—The expression and localization of

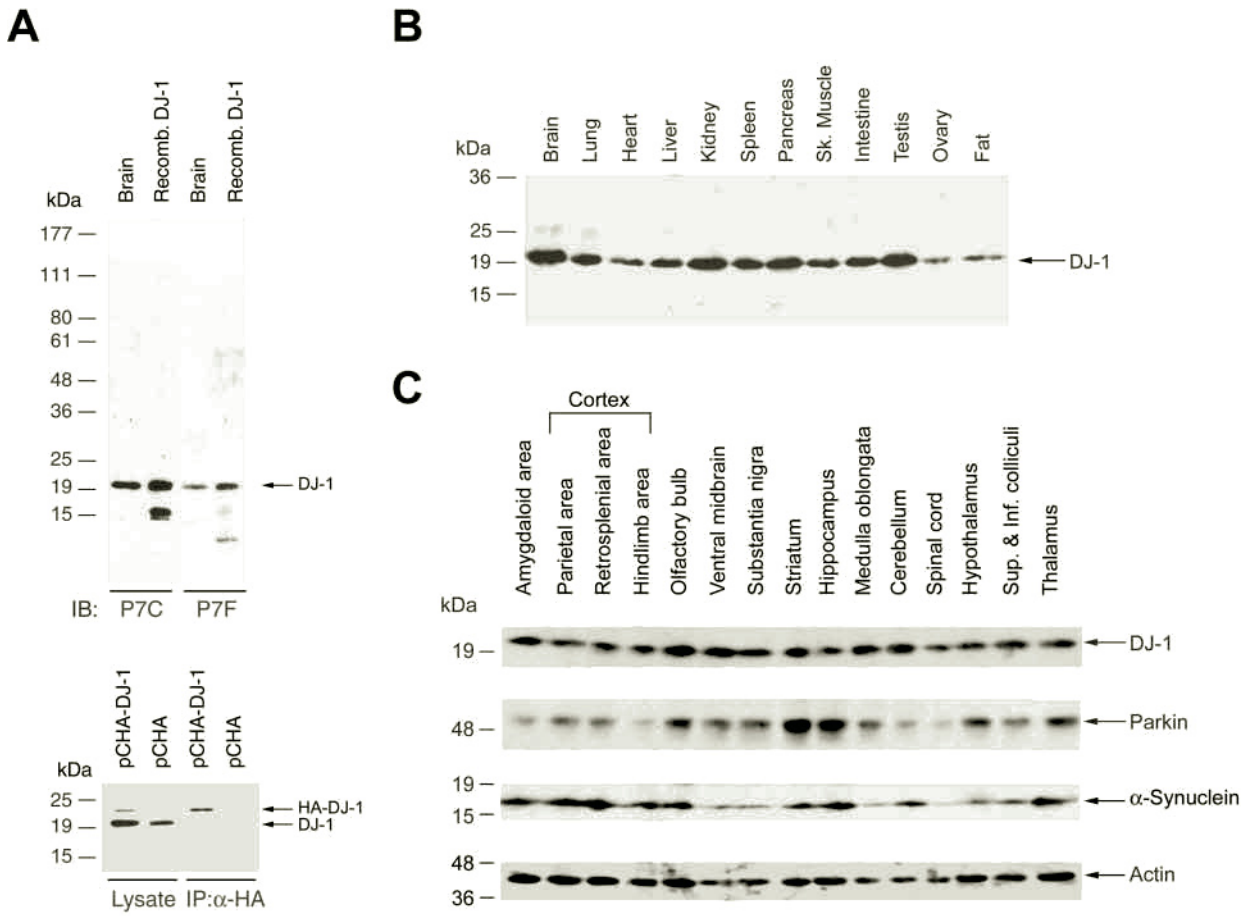

FIG. 1. **Expression and distribution of DJ-1 protein.** *A*, specificity of two novel polyclonal anti-DJ-1 antibodies, P7C and P7F. *Upper panel*, Western blot analysis of rat brain homogenate and untagged, recombinant (*Recomb.*) DJ-1 protein expressed in *E. coli* cells using anti-DJ-1 antibody P7C or P7F. *Lower panel*, cell lysates prepared from HeLa cells transfected with pCHA-DJ-1 or pCHA vector control were immunoprecipitated with anti-HA antibody followed by immunoblotting with anti-DJ-1 antibody P7C. *IB*, immunoblot; *IP*, immunoprecipitation. *B*, tissue distribution of DJ-1 protein expression. Equal amounts of homogenates (60 μg of protein/lane) from the indicated rat tissues were analyzed by immunoblotting using anti-DJ-1 antibody P7C. *Sk.*, skeletal. *C*, regional distribution of DJ-1 protein in rat brain compared with parkin and α-synuclein. Equal amounts of homogenates (50 μg of protein/lane) from the indicated brain tissues were immunoblotted for DJ-1, parkin, α-synuclein, and actin. *Sup.*, superior; *Inf.*, inferior. All data are representative of at least three independent experiments.

DJ-1 protein are poorly characterized, and virtually nothing is presently known about the distribution of DJ-1 protein in the nervous system. For characterization of DJ-1 at the protein level, we generated two distinct rabbit polyclonal anti-DJ-1 antibodies, P7F and P7C, against purified full-length recombinant protein and a carboxyl-terminal peptide of human DJ-1, respectively. Western blot analysis demonstrated that both anti-DJ-1 antibodies, but not their corresponding preimmune controls, recognized the 20-kDa endogenous DJ-1 protein as well as recombinant DJ-1 protein expressed in bacteria and mammalian cells (Fig. 1*A* and data not shown). Preabsorption of the P7F and P7C antibodies with purified recombinant DJ-1 protein completely eliminated their immunoreactivity to the recombinant as well as endogenous DJ-1 protein (data not shown), confirming the specificity of these antibodies. The lower molecular weight bands in the recombinant DJ-1 lanes are likely to be the proteolytic products of DJ-1 because they varied from blot to blot, and none of these bands were detected when the blots were analyzed with anti-DJ-1 antibodies preabsorbed with DJ-1 immunogens.

Using these anti-DJ-1 antibodies, we demonstrated that DJ-1 is ubiquitously expressed in all tissues tested with high expression levels in brain, testis, and kidney (Fig. 1*B*). To further characterize the expression of DJ-1 in brain, various brain regions were dissected from adult rats and subjected to Western blot analysis using the anti-DJ-1 antibodies. For comparison, we also analyzed the same samples with antibodies against parkin and α-synuclein. The result shows that these three PD-associated proteins are widely expressed throughout the brain with distinct distribution patterns (Fig. 1*C*). DJ-1 exhibits relatively higher protein expression levels in brain regions that are affected in Parkinson's disease, such as the substantia nigra or ventral midbrain area, compared with the levels in the hippocampus and cerebral cortical regions.

Immunolocalization of DJ-1 Protein in Rat Brain—We then used these anti-DJ-1 antibodies to determine the cellular distribution of DJ-1 protein in rat brain by immunohistochemistry. Consistent with the results of Western blot analysis (Fig. 1*C*), intense DJ-1 immunostaining was observed in the substantia nigra (Fig. 2*E*). Nearly all neurons, including dopaminergic neurons, in the pars compacta and pars reticulata of the substantia nigra contained DJ-1 immunoreactivity in their nuclei, perikarya, and processes. In the striatum, large interneurons were intensely stained for DJ-1, whereas the medium spiny neurons were moderately well stained (Fig. 2*D*).

In addition to the nigral-striatal system, DJ-1 immunoreactivity was widely distributed in many neurons throughout the brain. In the cerebral cortex, layer V pyramidal cells were

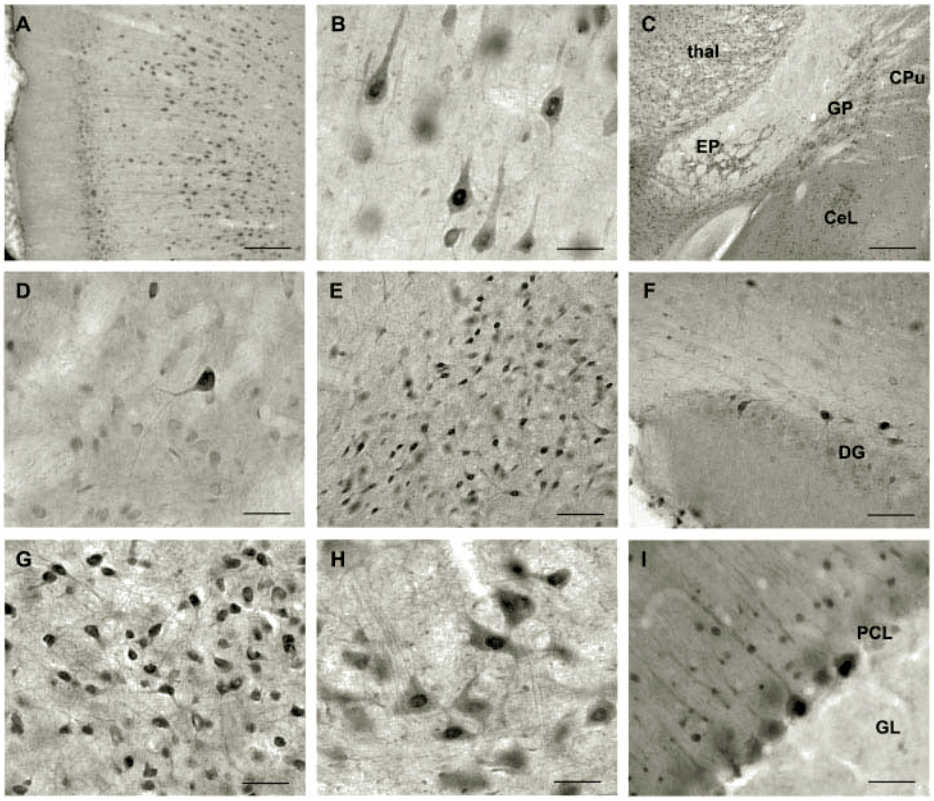

FIG. 2. **Immunohistochemical analysis of DJ-1 protein distribution in rat brain.** *A*, retrosplenial gyrus. *B*, layer V pyramidal neurons in frontal cortex. *C*, immunoreactive neurons are present throughout the thalamus (*thal*), entopeduncular nucleus (*EP*), and central amygdaloid nucleus (*CeL*). Globus pallidus (*GP*) is more strongly immunostained than the caudate-putamen (*CPu*). *D*, in the striatum, large interneurons are generally more prominently stained than medium spiny neurons. *E*, substantia nigra showing pars compacta (*middle*) and pars reticulata (*lower right corner*). *F*, hippocampal interneurons in the hilus of the dentate gyrus display DJ-1 immunostaining, whereas dentate granule cells (*DG*) do not. *G*, ventromedial nucleus of the hypothalamus. *H*, magnocellular neurons in the red nucleus. *I*, Purkinje cell layer (*PCL*) neurons display intense immunostaining in contrast to the granular layer (*GL*). Scale bar = 125 μm in *A*; 30 μm in *B*, *D*, *G*, *H*, and *I*; 500 μm in *C*; and 60 μm in *E* and *F*.

prominently stained in addition to moderately stained neurons in all lamina and in all cortical regions (Fig. 2, *A* and *B*). Intense DJ-1 immunostaining was present in the islands of Calleja, the diagonal band of Broca, piriform cortex, and septum. In the hippocampus, immunoreactivity was much greater in interneurons than in dentate gyrus granule cells (Fig. 2*F*). Neuronal labeling was also prominent in the entopeduncular and subthalamic nuclei, globus pallidus, and the basolateral and central amygdaloid nuclei (Fig. 2*C*); throughout the thalamus (Fig. 2*C*); in the ventromedial hypothalamic nucleus (Fig. 2*G*); and in magnocellular neurons of the red nucleus (Fig. 2*H*). In the cerebellum, there was strong immunoreactivity in Purkinje cells but not in granule cells (Fig. 2*I*). In brain stem, the motor nuclei of the oculomotor, trigeminal, and facial nerves and the nucleus ambiguus were intensely stained.

Within labeled neurons, DJ-1 immunostaining was localized in both nucleus and cytoplasm, including neuronal processes and neuropil. Prominent immunoreactive axons and dendrites were often seen extending over distances greater than 1 mm from the soma. In addition to neurons, DJ-1 immunostaining was also present in oligodendroglia, astrocytes, and cells of the pia mater, ventricular ependyma, and vascular endothelium, although these non-neuronal cells were weakly labeled. Similar staining patterns were obtained with two different anti-DJ-1 antibodies, P7F and P7C, indicating that the observed DJ-1 immunostaining is specific. The specificity of DJ-1 immunoreactivity was further confirmed by preabsorption experiments and in controls where anti-DJ-1 primary antibody was omitted (data not shown).

L166P Mutation Causes DJ-1 Protein to Unfold into a "Random Coil" Structure—To investigate structural consequences of PD-linked L166P mutation, we used circular dichroism spectroscopy to study the secondary structure of DJ-1 and its mutant proteins (Fig. 3*A*). At physiological pH, wild-type DJ-1 protein showed a CD spectrum with maximal negative ellipticity at 208 and 222 nm, indicating a substantial amount of α-helical content in the solution structure of DJ-1. Since the crystal structure of DJ-1 suggests that the highly conserved cysteine residue at position 106 may play a key role in DJ-1 catalytic function (25–28), we made the C106A mutant DJ-1 by replacing the Cys-106 residue with an alanine. The CD spectrum of the C106A mutant was virtually indistinguishable from that of wild-type DJ-1, indicating that the C106A mutation has no effect on the DJ-1 structure. In contrast, the L166P mutant DJ-1 protein exhibited a very different CD spectrum, showing large negative ellipticity at ~200 nm and small negative values in the 210–230-nm region. This CD spectrum indicates that the L166P mutant contains high content of random coil or unfolded structure and relatively little α-helical structure.

To assess the structural stability of DJ-1 and its mutants, we performed thermal denaturation experiments by monitoring ellipticity at 222 nm while the temperature was increased in steps from 5 °C to 90 °C (Fig. 3*B*). The results revealed that the folded structure of DJ-1 was relatively stable and underwent unfolding with a T_m of 72 °C. The unfolding was reversible as the CD spectra indicated that the denatured DJ-1 was able to refold upon stepwise cooling from 90 °C to 5 °C (data not shown). The C106A mutant behaved similarly to wild-type DJ-1 in the thermal unfolding and refolding experiments with a slightly decreased stability (Fig. 3*B* and data not shown). The CD spectra of heat-denatured wild-type and C106A mutant DJ-1 at 90 °C were almost indistinguishable from the spectrum of the L166P mutant at 25 °C (data not shown), further supporting the notion that the L166P mutant structure (Fig. 3*A*) represents an unfolded DJ-1 conformation. Thermal denaturation experiments revealed that the L166P mutant could not be further unfolded by increasing the temperature to 90 °C (Fig. 3*B*). The CD spectra of L166P mutant before and after boiling were virtually identical (data not shown), indicating that the random coil conformation of the L166P mutant is a stable structure. Furthermore the thermal refolding experiments showed that the L166P mutant was unable to fold into a wild-type DJ-1-like structure by stepwise lowering the temperature

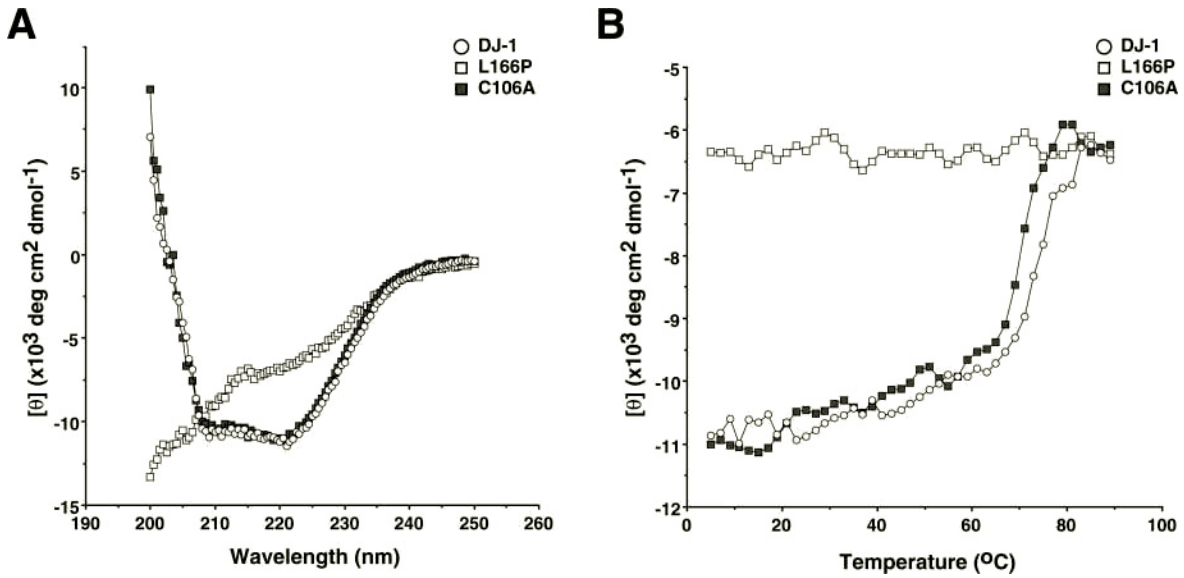

FIG. 3. **Far UV CD spectroscopic analysis of the secondary structure and thermal unfolding of DJ-1 and its mutants.** *A*, CD spectra of wild-type, L166P mutant, and C106A mutant DJ-1 proteins measured at 25 °C. *B*, thermal denaturation of DJ-1 and its mutants. Ellipticity was recorded at 222 nm at temperatures from 5 °C to 90 °C with 2 °C step increases. *deg*, degrees.

to 5 °C (data not shown). Together these data suggest that the L166P mutation impairs the intrinsic folding propensity of DJ-1 protein, resulting in a spontaneously unfolded structure.

L166P Mutant Is Incapable of Forming a Dimeric Structure in Vitro—Next we performed gel filtration experiments to compare the oligomeric state of wild-type and L166P mutant DJ-1. As shown in Fig. 4, recombinant DJ-1 protein eluted from the Sephacryl S-100 gel filtration column as a single peak with an apparent molecular mass of ~38 kDa, which is very close to the predicted molecular mass of 40 kDa for the dimeric form of DJ-1. By comparison, no L166P mutant DJ-1 protein was detected in the fractions corresponding to the size of the dimeric form. Instead a significant portion of L166P mutant protein was found in the fractions corresponding to the size of the monomeric form with an apparent molecular mass of ~19 kDa (Fig. 4), indicating that L166P mutant protein exists as a monomer instead of a dimer in solution. During the course of protein purification, we noted that the L166P mutant protein had a higher tendency to undergo aggregation compared with wild-type DJ-1. Consistent with this notion, a substantial amount of L166P mutant protein eluted in the void volume fractions (Fig. 4).

L166P Mutation Prevents the Assembly of the Homodimer and the DJ-1· L166P Heterodimer in Vivo—We then examined the *in vivo* self-association of DJ-1 and its L166P mutant and the interaction between wild-type and mutant DJ-1 by co-immunoprecipitation of differentially tagged wild-type and mutant DJ-1 proteins in HeLa cells. As shown in Fig. 5, Myc-tagged DJ-1 co-immunoprecipitated with HA-tagged DJ-1, indicating the presence of DJ-1 homodimers in mammalian cells. In contrast, Myc-tagged L166P mutant was unable to co-immunoprecipitate with either HA-tagged L166P mutant or with HA-tagged wild-type DJ-1, indicating that the L166P mutation not only disrupts the assembly of the homodimer but also prevents the formation of the heterodimer between wild-type and L166P mutant DJ-1. Unlike the L166P mutation, the C106A mutation did not affect the dimerization of DJ-1 (Fig. 5). By comparison, the C106A/L166P double mutation abolished the dimer formation, further confirming the inhibitory effect of L166P mutation on DJ-1 dimerization. Similar results were also obtained when the co-immunoprecipitation experiments were carried out with untagged or GFP-tagged wild-type and mutant DJ-1 proteins (data not shown).

DJ-1 Does Not Appear to Have a Molecular Chaperone Function—Elucidation of the biochemical function of DJ-1 is crucial for unraveling the molecular basis of PD pathogenesis. The significant sequence and structural homology between DJ-1 and *E. coli* chaperone protein Hsp31 (25, 41) raises an intriguing possibility that DJ-1 may function as a molecular chaperone. To test this possibility, we used a well established chaperone assay (33, 41) to determine whether DJ-1 has the ability to suppress the heat-induced aggregation of the chaperone substrate citrate synthase. As shown in Fig. 6*A*, light scattering measurement revealed that citrate synthase, when incubated at heat shock temperature (43 °C), underwent rapid aggregation with a time course consistent with previous reports (33, 41). By comparison, no detectable heat-induced aggregation of DJ-1 or its mutant forms (L166P or C106A) could be observed when these DJ-1 proteins were incubated alone at 43 °C (Fig. 6*A* and data not shown). The lack of heat-induced aggregation of wild-type and mutant DJ-1 is in agreement with the results (Fig. 3*B*) of thermal denaturation experiments measured by CD spectroscopy. As expected, the heat-induced aggregation of citrate synthase could be effectively suppressed by an equal molar amount of Hsp25, a known molecular chaperone (Fig. 6*A*). However, under the same experimental conditions, wild-type, L166P mutant, or C106A mutant DJ-1 protein was unable to inhibit the thermal aggregation of citrate synthase even when provided at 3-fold molar excess (Fig. 6*A*) or up to 20-fold molar excess over the substrate protein (data not shown). Similar negative results were obtained when the experiments were repeated in the presence of 300 μM H_2O_2 (data not shown), indicating that DJ-1 does not appear to have a chaperone function in this assay even under the oxidized conditions.

DJ-1 Functions as a Cysteine Protease—Since DJ-1 also shares significant sequence and structural homology with the PfpI family of intracellular proteases (23, 35), we sought to determine whether DJ-1 possesses intrinsic protease activity. We first assessed the proteolytic activity of DJ-1 by using the same in-gel protease assay that was used to demonstrate the protease activity of PfpI and PH1704 (34, 35). No detectable proteolytic activity could be observed for DJ-1 protein despite the robust proteolytic activity exhibited by the positive control trypsin (data not shown). The failure to detect DJ-1 protease activity in this assay could be due to the loss of DJ-1 quater-

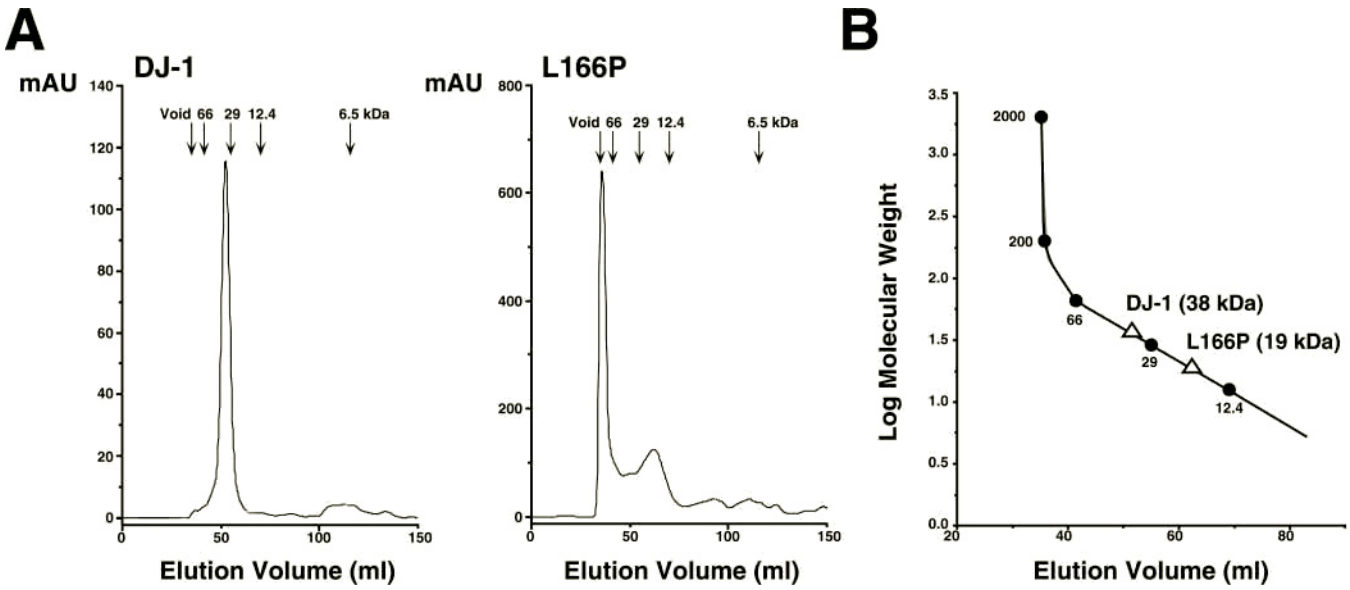

FIG. 4. **Gel filtration analysis of the oligomeric state of DJ-1 and its L166P mutant.** *A*, elution profile of wild-type DJ-1 (*left panel*) and L166P mutant DJ-1 (*right panel*) through a Sephacryl S-100 high-resolution gel filtration column. *mAU*, milliabsorbance units at 280 nm. *B*, plot of the observed elution of DJ-1 and L166P mutant protein against the calibration standard curve reveals that DJ-1 exists as a dimer (38 kDa), whereas L166P is a monomer (19 kDa) in solution. Standards used for column calibration are blue dextran (2000 kDa), β-amylase (200 kDa), albumin (66 kDa), carbonic anhydrase (29 kDa), cytochrome *c* (12.4 kDa), and aprotinin (6.5 kDa).

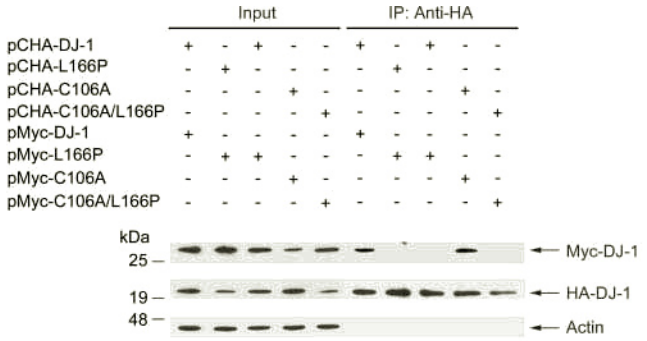

FIG. 5. **Homo- and hetero-oligomerization of DJ-1 and its mutants *in vivo*.** Lysates from HeLa cells transfected with the indicated plasmids encoding HA- or Myc-tagged wild-type DJ-1, L166P single mutant, C106A single mutant, or C106A/L166P double mutant were subjected to immunoprecipitation with anti-HA antibody. The HA- and Myc-tagged wild-type and mutant DJ-1 proteins in the lysates (*Input*) and immunoprecipitates were detected by immunoblotting. Control immunoblotting for actin confirms the specificity of the co-immunoprecipitations. All data are representative of at least three independent experiments. *IP*, immunoprecipitation.

nary and tertiary structure caused by SDS denaturation during gel electrophoresis.

We then used a highly sensitive, fluorescence-based protease assay (36) to investigate the potential protease activity of DJ-1. This assay allows continuous, real time measurement of protease activity by using the intramolecularly quenched BODIPY FL-labeled casein as the substrate. As shown in Fig. 6*B*, proteolysis of the quenched casein substrate by a protease such as trypsin releases highly fluorescent BODIPY FL-peptides, which can be detected as an increase in fluorescence. Incubation of purified recombinant DJ-1 with the quenched casein substrate also led to increases in fluorescence with time, indicating that DJ-1 possesses intrinsic proteolytic activity to hydrolyze the casein substrate. However, the concentrations of DJ-1 (*e.g.* 30 μM in Fig. 6*B*) needed to produce reasonable fluorescence increases were at least 3 orders of magnitude higher than the concentrations of trypsin (*e.g.* 0.1 μM in Fig. 6*B*), indicating that DJ-1 has a weak catalytic activity. Kinetic studies revealed that DJ-1-mediated casein proteolysis has a K_m value of 133 μM and a k_{cat} of 0.0057 s^{-1}, giving a catalytic efficiency (k_{cat}/K_m) of 43 M^{-1} s^{-1}, which is much lower than that observed for trypsin (250,000 M^{-1} s^{-1}). The proteolytic activity of DJ-1 was not significantly affected by 300 μM H_2O_2 (data not shown), arguing against the possibility that the DJ-1 protease function is activated in response to oxidative stress.

Based on the sequence and structural homology of DJ-1 with the PfpI family of intracellular proteases, it has been proposed that Cys-106 of DJ-1 may serve as the active site nucleophile for its catalytic function (25, 26, 28). To examine this possibility, we assessed the effect of mutation of Cys-106 to an Ala (C106A) on the protease activity of DJ-1. As shown in Fig. 6*B*, the C106A mutation completely abolished the proteolytic activity of DJ-1. Since the C106A mutation had little effect on the structure (Fig. 3) or dimerization of DJ-1 (Fig. 5), the lack of the proteolytic activity of the C106A mutant suggests an essential role for Cys-106 in the catalytic function of DJ-1. In addition, we found that the protease activity of DJ-1 is abolished by the PD-linked L166P mutation (Fig. 6*B*), demonstrating that L166P is a loss-of-function mutation.

L166P Mutant, but Not Wild-type DJ-1, Is Selectively Polyubiquitinated in Vivo—In cells, misfolded proteins are usually recognized and degraded by the ubiquitin-proteasome proteolytic pathway (42, 43). The ubiquitin-proteasome pathway consists of two major steps: the conjugation of ubiquitin to the substrate and subsequent degradation of the ubiquitinated substrate protein by the 26 S proteasome. Although the L166P mutant was recently suggested to undergo degradation by the ubiquitin-proteasome pathway (44), it remains to be determined experimentally whether the L166P mutant is indeed ubiquitinated. To address this issue, we used a well established *in vivo* ubiquitination assay (39, 45) to measure the ubiquitination of DJ-1 and its L166P mutant in mammalian cells. Lysates from HeLa cells expressing Myc-tagged ubiquitin in combination with HA-tagged wild-type or L166P mutant DJ-1 were subjected to immunoprecipitation with anti-HA antibodies followed by immunoblotting with anti-Myc antibodies to detect ubiquitin-conjugated DJ-1 proteins (Fig. 7). As expected, treatment of cells with the proteasome inhibitor MG132 resulted in accumulation of ubiquitinated substrate proteins

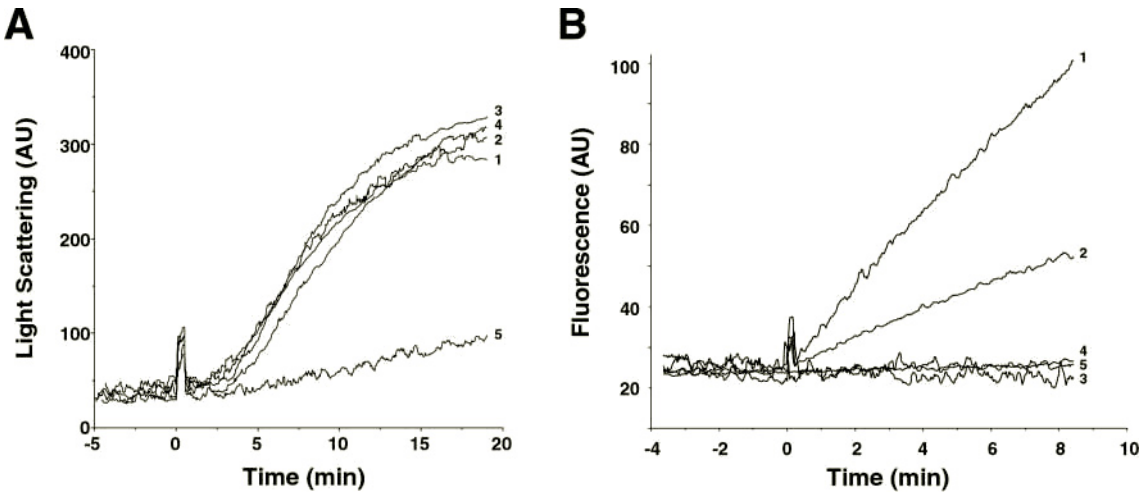

FIG. 6. **Functional characterization of the catalytic activity of DJ-1 and its mutants.** *A*, the potential chaperone activity of DJ-1 was assessed by the ability to suppress the aggregation of citrate synthase at 43 °C. Light scattering measurements of citrate synthase (0.15 μM) in the absence (*trace 1*) or presence of 0.45 μM wild-type human DJ-1 (*trace 2*), C106A mutant (*trace 3*), or L166P mutant DJ-1 (*trace 4*) or 0.15 μM murine Hsp25 (*trace 5*). *B*, the protease activity of DJ-1 was assessed by a continuous, real time fluorescence-based protease assay using BODIPY FL-casein as the substrate. Fluorometric recordings of 0.1 μM trypsin (*trace 1*) and 30 μM wild-type human DJ-1 (*trace 2*), C106A (*trace 3*), L166P mutant DJ-1 (*trace 4*), or bovine serum albumin (*trace 5*) are shown. *AU*, arbitrary units.

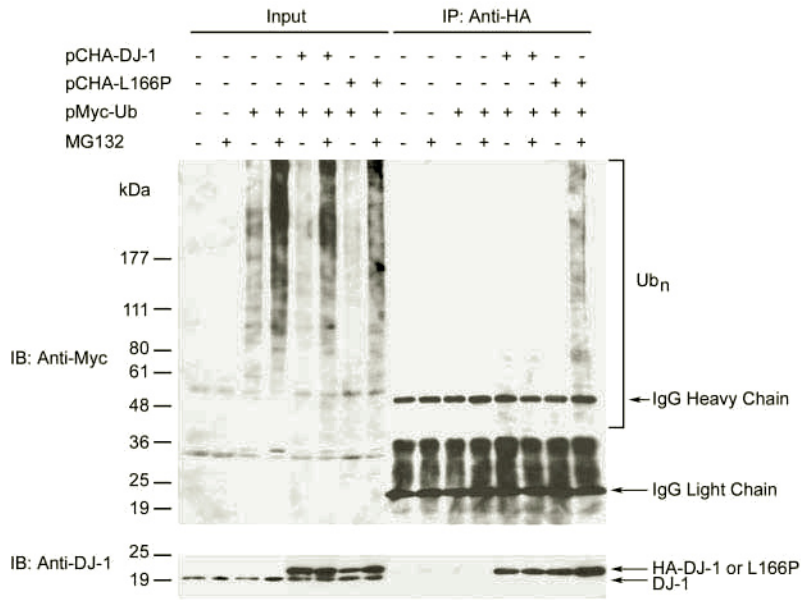

FIG. 7. **L166P mutant DJ-1 protein is polyubiquitinated in mammalian cells.** HeLa cells were transfected with the indicated plasmids and incubated in the absence or presence of proteasome inhibitor MG132 for 8 h before harvest. Cell lysates were subjected to immunoprecipitation with anti-HA antibody followed by immunoblotting with anti-Myc antibody to detect Myc-ubiquitin conjugated to DJ-1 proteins. The blot was then stripped and reprobed with anti-DJ-1 antibody P7C. *IP*, immunoprecipitation; *IB*, immunoblot; *Ub*, ubiquitin; *Ub$_n$*, polyubiquitin.

compared with vehicle-treated controls (Fig. 7, *Input lanes*). Immunoprecipitation results showed that only the L166P mutant, but not wild-type DJ-1, is ubiquitinated. The ubiquitination of the L166P mutant seems to be polyubiquitination because ubiquitinated L166P mutant proteins were only accumulated in the MG132-treated cells and appeared as a high molecular weight smear (Fig. 7).

Misfolded L166P Mutant Protein Is Degraded by the Proteasome—We then measured the stability and steady-state levels of wild-type and L166P mutant DJ-1 to determine whether the polyubiquitination of L166P mutant targets it for degradation by the 26 S proteasome. First we performed pulse-chase experiments to compare the turnover rate of HA-tagged DJ-1 and its L166P mutant in stably transfected human neuroblastoma SH-SY5Y cells. As shown in Fig. 8*A*, the half-life of wild-type DJ-1 was ~33 h, whereas the half-life of the L166P mutant was reduced to 1 h, indicating that the L166P mutant protein is considerably unstable compared with wild-type DJ-1. Consistent with this result, Western blot analysis revealed that the steady-state expression level of the L166P mutant was significantly lower compared with wild-type DJ-1 (Fig. 8*B*). The steady-state level of the L166P mutant was increased by treatment of cells with the proteasome inhibitor MG132 but not by treatment with the lysosomal protease inhibitor chloroquine (Fig. 8*B*). These results, together with the ubiquitination data (Fig. 7), provide strong support for a role of the L166P mutation in provoking the degradation of the mutant protein by the ubiquitin-proteasome pathway.

DISCUSSION

While monogenic familial forms of Parkinson's disease are rare, molecular studies of the underlying gene products responsible for these PD cases can provide novel insights into the pathogenic mechanisms of this devastating illness. To elucidate the role of DJ-1 in normal physiology and in PD pathogenesis, we generated two novel anti-DJ-1 antibodies and characterized DJ-1 protein expression by Western blot analysis and immunohistochemistry. Our results indicated that DJ-1 protein is abundantly expressed in rat brain where it is enriched in neurons. Consistent with previous studies in non-neuronal

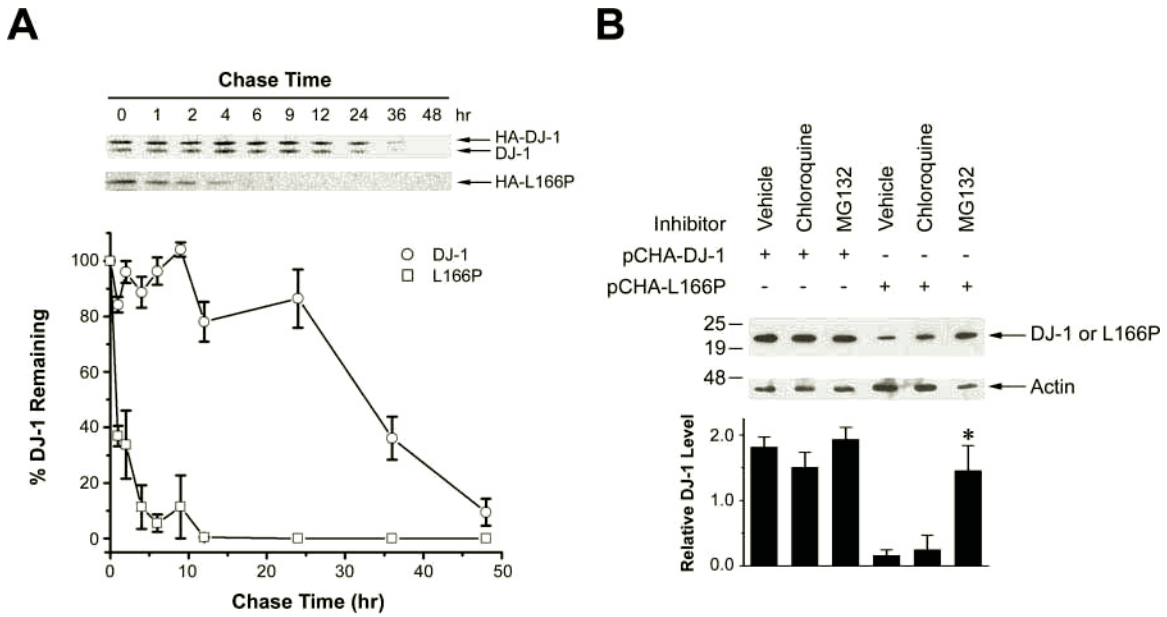

FIG. 8. **Polyubiquitination of L166P mutant DJ-1 targets it for degradation by the proteasome.** *A*, human neuroblastoma SH-SY5Y cells expressing HA-tagged wild-type or L166P mutant DJ-1 were pulse-labeled for 1 h with Dulbecco's modified Eagle's medium containing [^{35}S]Met/Cys, chased with non-radioactive Met/Cys for the indicated time, and then lysed. ^{35}S-Labled wild-type or mutant DJ-1 proteins were immunoprecipitated with anti-HA antibodies and detected by SDS-PAGE and autoradiography. The levels of HA-tagged wild-type or L166P mutant DJ-1 were quantified using a PhosphorImager and plotted as relative to the corresponding DJ-1 levels at 0 h. Data are shown as mean ± S.E. (*error bars*) of the results from at least three independent experiments. *B*, effect of L166P mutation on DJ-1 degradation was blocked by proteasome inhibitors. SH-SY5Y cells expressing HA-tagged wild-type or L166P mutant DJ-1 were incubated for 8 h at 37 °C with vehicle control (0.1% Me_2SO), 20 μM MG132, or 100 μM chloroquine. Cell lysates were analyzed by immunoblotting using antibodies against the HA tag or actin. The relative level of wild-type or mutant DJ-1 was measured by quantification of the intensity of the 20-kDa DJ-1 band and normalized to the actin level in the corresponding cell lysate. The *bar graph* shows the results (mean ± S.E.) from at least three independent experiments. The *asterisk* indicates a statistically significant ($p < 0.03$) increase in the level of L166P mutant DJ-1 in MG132-treated cells *versus* vehicle-treated controls.

cells (10, 12, 14), endogenous DJ-1 protein was localized to both nucleus and cytoplasm of neurons, suggesting that DJ-1 has a cytoplasmic and a nuclear function. The presence of DJ-1 in neuronal processes and neuropil suggests that DJ-1 may participate in neuronal and/or synaptic function. The abundant expression of DJ-1 in neurons vulnerable to PD (*e.g.* substantia nigra) supports a role for DJ-1 in PD pathogenesis. However, like other PD gene products such as α-synuclein and parkin, DJ-1 protein was not confined to these vulnerable neurons but rather was widely distributed throughout the brain. It is important to find out why loss-of-function mutations in DJ-1 cause selective neurodegeneration in the substantia nigra.

By using gel filtration chromatography and co-immunoprecipitation analysis, we showed that DJ-1 exists as a dimer in solution, which is in agreement with recent reports (26, 27, 44). Our circular dichroism spectroscopic analyses revealed that, consistent with the crystal structure, the solution structure of DJ-1 contains substantial amount of α-helical structure. The CD data indicated that the solution structure of DJ-1 is a stable structure that unfolds with a melting temperature of 72 °C. Since the gel filtration profile and the CD spectrum of DJ-1 were unaltered by a 10-fold dilution of the DJ-1 protein concentrations used in these analyses (data not shown), it appears that the DJ-1 dimer does not easily dissociate into monomers. The lack of a monomer peak in the gel filtration profile of DJ-1 suggests that DJ-1 does not exist in monomer-dimer equilibrium in solution.

The crystal structure of DJ-1 reveals a high degree of structural similarity between DJ-1 and the bacterial protease PH1704 and *E. coli* chaperone protein Hsp31 (25–29). However, unlike PH1704 and Hsp31, DJ-1 does not have a Cys-His-(Glu/Asp) catalytic triad. Instead DJ-1 contains the putative nucleophile Cys-106, which has the potential to form a Cys-His diad. The lack of a complete catalytic triad implies that DJ-1 may not have a protease function, a hypothesis that seemed to be supported by the failure to detect the protease activity of DJ-1 in assays using bovine serum albumin or azocasein as the substrate (27, 29). On the other hand, it has been proposed that DJ-1 may have a protease function by using the Cys-His diad as the catalytic mechanism (26). A fully functional Cys-His catalytic diad has been demonstrated in several cysteine proteases, such as the caspases (46, 47). Interestingly, by using a fluorescence-based protease assay that is at least 100 times more sensitive than the bovine serum albumin or azocasein assay (36), we were able to demonstrate that purified recombinant DJ-1 protein possesses intrinsic protease activity. This activity was completely abolished by the mutation of Cys-106 to an Ala, providing strong support for the function of DJ-1 as a cysteine protease.

Our kinetic studies revealed that the catalytic efficiency (k_{cat}/K_m) of purified DJ-1 protein is very low (43 M^{-1} s^{-1}) compared with trypsin, but it is comparable to the k_{cat}/K_m values reported for purified herpes simplex virus-1 protease (38 M^{-1} s^{-1}) and adenovirus protease (24 M^{-1} s^{-1}) (48, 49). The low catalytic efficiency of DJ-1 could be due to the fact that the BODIPY FL-casein is a poor substrate for DJ-1, and it is possible that DJ-1 may exhibit much higher catalytic efficiency toward its endogenous substrates. In addition, there may be a cellular cofactor(s) or other activation mechanism(s) for increasing the catalytic efficiency of the DJ-1 protease *in vivo*. Identification of such cofactors and endogenous substrates would be crucial steps toward a mechanistic understanding of DJ-1 action in normal physiology and in PD pathogenesis.

Because DJ-1 exhibits significant sequence and structural homology to *E. coli* chaperone protein Hsp31, we tested whether purified recombinant DJ-1 protein possesses intrinsic chaperone activity. Although the positive control Hsp25 exhibited robust chaperone activity in suppressing the heat-induced

aggregation of the chaperone substrate citrate synthase, our chaperone assays failed to detect any chaperone activity for purified DJ-1. This result is in contrast with a recent report (29) showing that DJ-1 has chaperone activity in suppressing the heat-induced aggregation of citrate synthase. The reason for this discrepancy is unclear. Since we obtained negative chaperone activity results for different batches of purified DJ-1 and since we showed that the purified DJ-1 retained its intact conformation and exhibited protease activity, it seems unlikely that the chaperone activity of DJ-1 is lost during purification.

In this study, we also investigated the structural and functional consequences of PD-linked L166P DJ-1 mutation. In the crystal structure of wild-type DJ-1, Leu-166 is located in the middle of helix H7, which, together with helix H8, mediates the dimerization of DJ-1. Based on this information, it was postulated that mutation of Leu-166 to Pro may act as a helix breaker to bend helix H7, thus perturbing the packing interactions at the dimer interface, leading to the disruption of the DJ-1 dimer (10, 25–29). The evidence presented here indicates that the structural consequence of the L166P mutation is much more severe than simply disrupting the DJ-1 dimerization or quaternary structure. Our CD results suggest that the L166P mutation impairs the intrinsic folding propensity of DJ-1 protein, resulting in the formation of a spontaneously unfolded protein with a random coil conformation. The disordered structure of the L166P mutant protein provides an explanation for the failure to obtain the crystal of the L166P mutant (25, 26).

Recently it was reported that the L166P mutation significantly reduces the signal in yeast two-hybrid interaction assays, although it is unclear whether the lack of signal is due to a reduced capacity for self-association or due to lower expression levels of the L166P mutant protein in yeast (44). In contrast, gel filtration analysis of lysates from L166P mutant-expressing cells showed that the mutant protein eluted in the fractions with a higher molecular mass (~68 kDa) than a dimer (~40 kDa), suggesting that the mutant forms either a "higher order" homo-oligomer or a complex with an unidentified protein (50). To clarify the effect of the L166P mutation on the oligomeric state and self-association of DJ-1, we performed gel filtration experiments with purified recombinant proteins and co-immunoprecipitation studies in transfected cells. Our results indicated that the L166P mutant protein is monomeric in solution, incapable of self-associating into a homo-oligomeric structure. Moreover the L166P mutant protein is incapable of interacting with wild-type DJ-1 to form a heterodimer. These results, together with our CD data, suggest that the inability of the L166P mutant protein to form a homodimer or a heterodimer is a direct consequence of impaired DJ-1 protein folding caused by the PD-linked point mutation. The inability of the L166P mutant to interact with wild-type DJ-1 is interesting because it predicts that, in human subjects with heterozygous L166P mutation, the L166P mutant does not act in a dominant negative manner to inhibit normal DJ-1 function by sequestering wild-type DJ-1 protein. This prediction is consistent with the observation that only the homozygous L166P mutation carrier exhibits Parkinsonian symptoms (10).

Our study demonstrated that the L166P mutation not only disrupted the structure of DJ-1 but also abolished the protease function of DJ-1. Moreover the L166P mutant, but not wild-type DJ-1, was selectively polyubiquitinated and subsequently degraded by the 26 S proteasome. How the L166P mutant protein is specifically recognized and earmarked for ubiquitin-mediated proteolysis is unclear. One possibility is that the L166P mutation-induced misfolding of DJ-1 protein leads to exposure of cryptic ubiquitination/degradation signals. The nature of such signals is unknown, but it has been proposed that exposed hydrophobic domains normally buried in the interior of the protein or in the protein-protein interaction interfaces may serve as recognition signals for the ubiquitination machinery (42, 43, 51). Interestingly recent evidence indicates that the PD-associated E3 ubiquitin-protein ligase parkin may facilitate the ubiquitination and degradation of misfolded proteins such as Pael-R and the polyglutamine-containing proteins in conjunction with the molecular chaperone Hsp70 and its binding partner carboxyl terminus of Hsp70-interacting protein (52–54). It would be worthwhile to determine whether parkin has a role in facilitating the ubiquitination of the L166P mutant DJ-1 protein.

The L166P mutation has been proposed to have the simple effect of promoting DJ-1 degradation, thereby functionally mimicking the deletion mutation in reducing net DJ-1 protein within the cell (44, 50). In contrast to this proposal, our results indicated that the fundamental effect of the L166P mutation is the disruption of DJ-1 protein folding, resulting in a spontaneously unfolded protein that is incapable of carrying out its catalytic function. Thus, the L166P mutation is a *bona fide* loss-of-function mutation. We have presented evidence supporting a function of DJ-1 as a cysteine protease, although DJ-1 may require a cofactor or other activation mechanism to make it more catalytically efficient. A protease function of DJ-1 would put DJ-1 in a similar pathogenic pathway as other familial PD gene products (α-synuclein, parkin, and ubiquitin carboxyl-terminal hydrolase L1) and support the hypothesis that dysfunction in protein degradation is a common cause for PD. Further investigation of the biochemical function of DJ-1 should lead to a better understanding of the pathogenic mechanisms underlying PD.

REFERENCES

1. Lang, A. E., and Lozano, A. M. (1998) *N. Engl. J. Med.* **339,** 1044–1053
2. Lang, A. E., and Lozano, A. M. (1998) *N. Engl. J. Med.* **339,** 1130–1143
3. Gwinn-Hardy, K. (2002) *Mov. Disord.* **17,** 645–656
4. Dawson, T. M., and Dawson, V. L. (2003) *J. Clin. Investig.* **111,** 145–151
5. Spillantini, M. G., Schmidt, M. L., Lee, V. M., Trojanowski, J. Q., Jakes, R., and Goedert, M. (1997) *Nature* **388,** 839–840
6. Kitada, T., Asakawa, S., Hattori, N., Matsumine, H., Yamamura, Y., Minoshima, S., Yokochi, M., Mizuno, Y., and Shimizu, N. (1998) *Nature* **392,** 605–608
7. Leroy, E., Boyer, R., Auburger, G., Leube, B., Ulm, G., Mezey, E., Harta, G., Brownstein, M. J., Jonnalagada, S., Chernova, T., Dehejia, A., Lavedan, C., Gasser, T., Steinbach, P. J., Wilkinson, K. D., and Polymeropoulos, M. H. (1998) *Nature* **395,** 451–452
8. McNaught, K. S., and Olanow, C. W. (2003) *Ann. Neurol.* **53,** S73–S86
9. Giasson, B. I., Lee, V. M., Ravina, B., Gwinn-Hardy, K., Crawley, A., St. George-Hyslop, P. H., Lang, A. E., Heutink, P., Bonifati, V., Hardy, J., Singleton, A., Wilson, M. A., Collins, J. L., Hod, Y., Ringe, D., and Petsko, G. A. (2003) *Cell* **114,** 1–8
10. Bonifati, V., Rizzu, P., van Baren, M. J., Schaap, O., Breedveld, G. J., Krieger, E., Dekker, M. C., Squitieri, F., Ibanez, P., Joosse, M., van Dongen, J. W., Vanacore, N., van Swieten, J. C., Brice, A., Meco, G., van Duijn, C. M., Oostra, B. A., and Heutink, P. (2003) *Science* **299,** 256–259
11. Hague, S., Rogaeva, E., Hernandez, D., Gulick, C., Singleton, A., Hanson, M., Johnson, J., Weiser, R., Gallardo, M., Ravina, B., Gwinn-Hardy, K., Crawley, A., St. George-Hyslop, P. H., Lang, A. E., Heutink, P., Bonifati, V., Hardy, J., Wilson, M. A., Collins, J. L., Hod, Y., Ringe, D., and Petsko, G. A. (2003) *Ann. Neurol.* **54,** 271–274
12. Nagakubo, D., Taira, T., Kitaura, H., Ikeda, M., Tamai, K., Iguchi-Ariga, S. M., and Ariga, H. (1997) *Biochem. Biophys. Res. Commun.* **231,** 509–513
13. Le Naour, F., Misek, D. E., Krause, M. C., Deneux, L., Giordano, T. J., Scholl, S., and Hanash, S. M. (2001) *Clin. Cancer Res.* **7,** 3328–3335
14. Hod, Y., Pentyala, S. N., Whyard, T. C., and El-Maghrabi, M. R. (1999) *J. Cell Biochem.* **72,** 435–444
15. Wagenfeld, A., Gromoll, J., and Cooper, T. G. (1998) *Biochem. Biophys. Res. Commun.* **251,** 545–549
16. Welch, J. E., Barbee, R. R., Roberts, N. L., Suarez, J. D., and Klinefelter, G. R. (1998) *J. Androl.* **19,** 385–393
17. Klinefelter, G. R., Laskey, J. W., Ferrell, J., Suarez, J. D., and Roberts, N. L. (1997) *J. Androl.* **18,** 139–150
18. Klinefelter, G. R., Welch, J. E., Perreault, S. D., Moore, H. D., Zucker, R. M., Suarez, J. D., Roberts, N. L., Bobseine, K., and Jeffay, S. (2002) *J. Androl.* **23,** 48–63
19. Takahashi, K., Taira, T., Niki, T., Seino, C., Iguchi-Ariga, S. M., and Ariga, H. (2001) *J. Biol. Chem.* **276,** 37556–37563
20. Niki, T., Takahashi-Niki, K., Taira, T., Iguchi-Ariga, S. M., and Ariga, H. (2003) *Mol. Cancer Res.* **1,** 247–261
21. Mitsumoto, A., Nakagawa, Y., Takeuchi, A., Okawa, K., Iwamatsu, A., and Takanezawa, Y. (2001) *Free Radic. Res.* **35,** 301–310

22. Mitsumoto, A., and Nakagawa, Y. (2001) *Free Radic. Res.* **35,** 885–893
23. Halio, S. B., Blumentals, I. I., Short, S. A., Merrill, B. M., and Kelly, R. M. (1996) *J. Bacteriol.* **178,** 2605–2612
24. Mizote, T., Tsuda, M., Smith, D. D., Nakayama, H., and Nakazawa, T. (1999) *Microbiology* **145,** 495–501
25. Huai, Q., Sun, Y., Wang, H., Chin, L. S., Li, L., Robinson, H., and Ke, H. (2003) *FEBS Lett.* **549,** 171–175
26. Tao, X., and Tong, L. (2003) *J. Biol. Chem.* **278,** 31372–31379
27. Wilson, M. A., Collins, J. L., Hod, Y., Ringe, D., and Petsko, G. A. (2003) *Proc. Natl. Acad. Sci. U. S. A.* **100,** 9256–9261
28. Honbou, K., Suzuki, N. N., Horiuchi, M., Niki, T., Taira, T., Ariga, H., and Inagaki, F. (2003) *J. Biol. Chem.* **278,** 31380–31384
29. Lee, S. J., Kim, S. J., Kim, I. K., Ko, J., Jeong, C. S., Kim, G. H., Park, C., Kang, S. O., Suh, P. G., Lee, H. S., and Cha, S. S. (2003) *J. Biol. Chem.* **278,** 44552–44559
30. Li, L., Schuchard, M., Palma, A., Pradier, L., and McNamee, M. G. (1990) *Biochemistry* (*Mosc.*) **29,** 5428–5436
31. Chin, L. S., Nugent, R. D., Raynor, M. C., Vavalle, J. P., and Li, L. (2000) *J. Biol. Chem.* **275,** 1191–1200
32. Li, Y., Chin, L. S., Weigel, C., and Li, L. (2001) *J. Biol. Chem.* **276,** 40824–40833
33. Buchner, J., Grallert, H., and Jakob, U. (1998) *Methods Enzymol.* **290,** 323–338
34. Blumentals, I. I., Robinson, A. S., and Kelly, R. M. (1990) *Appl. Environ. Microbiol.* **56,** 1992–1998
35. Du, X., Choi, I. G., Kim, R., Wang, W., Jancarik, J., Yokota, H., and Kim, S. H. (2000) *Proc. Natl. Acad. Sci. U. S. A.* **97,** 14079–14084
36. Jones, L. J., Upson, R. H., Haugland, R. P., Panchuk-Voloshina, N., Zhou, M., and Haugland, R. P. (1997) *Anal. Biochem.* **251,** 144–152
37. Batra, R., Khayat, R., and Tong, L. (2001) *Nat. Struct. Biol.* **8,** 810–817
38. Chin, L.-S., Raynor, M. C., Wei, X., Chen, H., and Li, L. (2001) *J. Biol. Chem.* **276,** 7069–7078
39. Wheeler, T. C., Chin, L. S., Li, Y., Roudabush, F. L., and Li, L. (2002) *J. Biol. Chem.* **277,** 10273–10282
40. Chin, L.-S., Vavalle, J. P., and Li, L. (2002) *J. Biol. Chem.* **277,** 35071–35079
41. Sastry, M. S., Korotkov, K., Brodsky, Y., and Baneyx, F. (2002) *J. Biol. Chem.* **277,** 46026–46034
42. Wilkinson, K. D. (2000) *Semin. Cell Dev. Biol.* **11,** 141–148
43. Glickman, M. H., and Ciechanover, A. (2002) *Physiol. Rev.* **82,** 373–428
44. Miller, D. W., Ahmad, R., Hague, S., Baptista, M. J., Canet-Aviles, R., McLendon, C., Carter, D. M., Zhu, P. P., Stadler, J., Chandran, J., Klinefelter, G. R., Blackstone, C., and Cookson, M. R. (2003) *J. Biol. Chem.* **278,** 36588–36595
45. Ellison, M. J., and Hochstrasser, M. (1991) *J. Biol. Chem.* **266,** 21150–21157
46. Wilson, K. P., Black, J. A., Thomson, J. A., Kim, E. E., Griffith, J. P., Navia, M. A., Murcko, M. A., Chambers, S. P., Aldape, R. A., Raybuck, S. A., and Livingston, D. J. (1994) *Nature* **370,** 270–275
47. Walker, N. P., Talanian, R. V., Brady, K. D., Dang, L. C., Bump, N. J., Ferenz, C. R., Franklin, S., Ghayur, T., Hackett, M. C., and Hammill, L. D. (1994) *Cell* **78,** 343–352
48. Darke, P. L., Chen, E., Hall, D. L., Sardana, M. K., Veloski, C. A., LaFemina, R. L., Shafer, J. A., and Kuo, L. C. (1994) *J. Biol. Chem.* **269,** 18708–18711
49. McGrath, W. J., Baniecki, M. L., Li, C., McWhirter, S. M., Brown, M. T., Toledo, D. L., and Mangel, W. F. (2001) *Biochemistry* (*Mosc.*) **40,** 13237–13245
50. Macedo, M. G., Anar, B., Bronner, I. F., Cannella, M., Squitieri, F., Bonifati, V., Hoogeveen, A., Heutink, P., and Rizzu, P. (2003) *Hum. Mol. Genet.* **12,** 2807–2816
51. McClellan, A. J., and Frydman, J. (2001) *Nat. Cell Biol.* **3,** E51–E53
52. Imai, Y., Soda, M., Inoue, H., Hattori, N., Mizuno, Y., and Takahashi, R. (2001) *Cell* **105,** 891–902
53. Imai, Y., Soda, M., Hatakeyama, S., Akagi, T., Hashikawa, T., Nakayama, K. I., and Takahashi, R. (2002) *Mol. Cell* **10,** 55–67
54. Tsai, Y. C., Fishman, P. S., Thakor, N. V., and Oyler, G. A. (2003) *J. Biol. Chem.* **278,** 22044–22055